J Ind Microbiol Biotechnol (2014) 41:1391–1404
DOI 10.1007/s10295-014-1489-1

SIMB
Society for Industrial Microbiology and Biotechnology

Use of a stress-minimisation paradigm in high cell density fed-batch *Escherichia coli* fermentations to optimise recombinant protein production

Chris Wyre · Tim W. Overton

Received: 26 March 2014 / Accepted: 8 July 2014 / Published online: 24 July 2014

Abstract Production of recombinant proteins is an industrially important technique in the biopharmaceutical sector. Many recombinant proteins are problematic to generate in a soluble form in bacteria as they readily form insoluble inclusion bodies. Recombinant protein solubility can be enhanced by minimising stress imposed on bacteria through decreasing growth temperature and the rate of recombinant protein production. In this study, we determined whether these stress-minimisation techniques can be successfully applied to industrially relevant high cell density *Escherichia coli* fermentations generating a recombinant protein prone to forming inclusion bodies, CheY–GFP. Flow cytometry was used as a routine technique to rapidly determine bacterial productivity and physiology at the single cell level, enabling determination of culture heterogeneity. We show that stress minimisation can be applied to high cell density fermentations (up to a dry cell weight of >70 g L^{-1}) using semi-defined media and glucose or glycerol as carbon sources, and using early or late induction of recombinant protein production, to produce high yields (up to 6 g L^{-1}) of aggregation-prone recombinant protein in a soluble form. These results clearly demonstrate that stress minimisation is a viable option for the optimisation of high cell density industrial fermentations for the production of high yields of difficult-to-produce recombinant proteins, and present a workflow for the application of stress-minimisation techniques in a variety of fermentation protocols.

Keywords Green fluorescent protein · Fed-batch fermentation · Flow cytometry · Inclusion bodies

Electronic supplementary material The online version of this article (doi:10.1007/s10295-014-1489-1) contains supplementary material, which is available to authorized users.

C. Wyre · T. W. Overton (✉)
Bioengineering, School of Chemical Engineering, and Institute of Microbiology and Infection, University of Birmingham, Edgbaston, Birmingham B15 2TT, UK
e-mail: t.w.overton@bham.ac.uk

Introduction

Production of recombinant proteins in bacterial hosts is an important part of the biopharmaceutical industry. Although many new biopharmaceutical drugs (such as monoclonal antibodies) are made in mammalian hosts, bacterial hosts are undergoing a resurgence in popularity not only for relatively simple protein and peptide drugs (such as insulin) but also for more complex molecules such as antibody fragments. Of the 58 biopharmaceutical drugs approved between 2006 and June 2010, 17 were produced in *Escherichia coli* [29]. Efficient production of soluble recombinant proteins is also essential for generation of proteins for structural studies that are the basis of the development of new drug ligand molecules.

Two major routes are utilised for recombinant protein production in bacterial hosts. First, the recombinant protein can be generated in the form of inclusion bodies (IBs); dense intracellular particles comprising mainly misfolded protein but also containing some correctly folded functional protein [6]. Many recombinant proteins have a tendency to form IBs in bacterial hosts for a number of reasons including differences in folding pathways and physicochemical conditions between bacteria and eukaryotic cells [14]. Inclusion bodies are relatively simple to generate to high yields, are easy to purify due to their density, and are a relatively pure source of recombinant protein [21]. However, to generate functional protein, IBs must be denatured (usually

chemically) and then the protein must be refolded; this refolding step varies in success and yield, such that some recombinant proteins cannot be successfully refolded.

Alternatively, the recombinant protein may be synthesised in a correctly folded, soluble form, and purified in this functional form [22]. This is especially desirable for recombinant proteins with multiple isoforms and for structural determination studies. However, there are many potential problems with this approach, and some recombinant proteins cannot be readily synthesised in bacteria in a soluble form. Often, attempts to produce soluble recombinant protein lead to IB formation, decreases in host cell viability, loss of recombinant protein-encoding plasmids and overgrowth of non-producing, plasmid-free bacteria, all of which can lead to low biomass and recombinant protein yields. Indeed, many recombinant proteins that are difficult to produce are referred to as 'toxic' proteins, due to the apparently toxic effects on host bacteria [17]. Nonetheless, soluble production frequently represents a desirable recombinant protein production route.

Previous studies have attempted to increase the proportion of soluble recombinant protein generated in bacterial hosts using a variety of methods. Some recombinant proteins can be induced to fold using modulation of chaperones, a class of proteins that assist protein folding (reviewed by [10]). This can be done by individual chaperone overproduction or induction of the heat shock response, the mechanism by which *E. coli* naturally responds to misfolded proteins; however, this route is far from generic and needs to be individually tested and optimised for each recombinant protein and host.

Another, more generically applicable, approach to increasing recombinant protein folding is minimisation of stress, typified by reducing the rate of recombinant protein production thus allowing recombinant protein translation and folding to proceed more slowly. Examples are the use of *E. coli* strains that transcribe recombinant protein-encoding genes more slowly [11] and reduction of inducer concentration and temperature [20]. In the latter system, two important improvements were made to fermentation conditions using the IPTG-induced pET system [24] to produce an aggregation-prone recombinant protein (CheY–GFP) in a soluble form. First, an IPTG concentration of 8 μM was used instead of 0.5 mM, which decreased the rates of CheY–GFP transcription and translation. Second, a growth temperature of 25 °C was used throughout the process instead of growth at 37 °C before induction of recombinant protein production and 25 °C after induction, to slow growth and translation rates and prevent cold shock. Although these alterations decreased the rate of recombinant protein synthesis, the reduction in physiological stress imposed on the bacteria meant that plasmid loss was greatly reduced, so far fewer bacteria were non-productive, and the slower rate of synthesis meant that CheY–GFP could be folded into a soluble form, decreasing IB formation. Overall, this 'improved' protocol resulted in far higher overall recombinant protein yields per unit biomass and higher recombinant protein solubility.

In order that such methods are useful industrially, they need to be applied to high cell density fermentation regimes such as fed-batch growth. In this study, we developed high cell density fed-batch fermentations using stress-minimisation methods [20] to achieve four aims: high biomass generation; high percentage of productive bacteria; high yield of recombinant protein; and enhanced solubility of the generated recombinant protein. We used flow cytometry (FCM) as a single-cell analysis tool to optimise the fermentations in terms of bacterial physiology and productivity. Protocols were developed that tested industrially derived semi-defined medium, different carbon sources, and different points of induction of recombinant protein production.

Materials and methods

Bacterial strains, plasmids, and microbiological methods

Escherichia coli strain BL21* (DE3) [F^- *ompT hsdS*$_B$ ($r_B^- m_B^-$) *gal dcm rne131* λ(DE3)] was used throughout (Invitrogen, Paisley, UK). The recombinant CheY–GFP fusion protein was encoded by the pET20bhc–CheY–GFP plasmid [8, 20], comprising the *E. coli cheY* gene fused to *gfp* cloned into pET20bhc [7, 27]. The *gfp* gene contains the S65T (maximum λ_{ex} red-shifted to 488 nm) and F64L (folding improvement) mutations and so is equivalent to the GFPmut1 protein [4]. Bacteria were transformed with the plasmid using the heat shock method and transformants selected on nutrient agar (Oxoid) plates supplemented with 100 μg carbenicillin mL^{-1} (Melford, Ipswich, UK; a more stable variant of ampicillin). Optical density at 650 nm was used as a routine measurement technique for biomass, due to its widespread use industrially and speed of data acquisition. For colony forming unit (CFU) analysis, bacterial cultures were serially decimally diluted in PBS (8 g L^{-1} NaCl, 0.2 g L^{-1} KCl, 1.15 g L^{-1} Na_2HPO_4, 0.2 g L^{-1} KH_2PO_4, pH 7.3; Oxoid), plated onto nutrient agar plates (Oxoid) and incubated at 25 °C for 48 h. Colonies were replica plated onto plates containing 80 μg carbenicillin mL^{-1} to determine plasmid retention. The dry cell weight (DCW) of four aliquots of 2 mL of culture (harvested by centrifugation) was determined after drying at 100 °C for ≥24 h.

Fermentation methods

An Electrolab (Tewkesbury, UK) Fermac 310/60 5 L bioreactor was used with four baffles and an agitator with 2

six-bladed Rushton turbines. Aeration was achieved by sparging air from below the lower impeller at a rate of 3 L min^{-1} through a reusable, autoclavable 0.22 μm filter (Sartorius). Dissolved oxygen tension (DOT) was measured in situ using a D150 Oxyprobe (Broadley James) and was maintained above a set point of 30 % by increasing agitation to a maximum of 1,000 rpm from a minimum of 200–500 rpm. pH was measured by an F-695 FermProbe (Broadley James) and was controlled at a set point of 6.3 ± 0.1 with the automated addition of sterile 10 % (v/v) NH_3 or 5 % (v/v) HCl. Off gas was passed through a condenser, autoclavable 0.22 μm filter (Sartorius), two catch pots and analysed using a PrimaDB gas mass spectrometer (Thermo); data were logged and analysed using GasWorks v1.0 (Thermo).

Inocula were grown from a sweep of cells from an agar plate in 35 mL of LB [10 g L^{-1} tryptone (BD Bacto), 5 g L^{-1} yeast extract (BD Bacto), 5 g L^{-1} NaCl (Sigma)] supplemented with 100 μg mL^{-1} carbenicillin in a 250 mL conical flask, at 25 °C and agitated at 150 rpm for 18–21 h. Prior to addition to the vessel, 5 mL of inoculum was removed and used for screening and analysis.

Five fermentation protocols were used as outlined in Table 1; the initial batch medium volume was 1.5 L in each case. Protocol A used a complex LB-based medium [20]: 10 g L^{-1} tryptone (BD Bacto), 5 g L^{-1} yeast extract (BD Bacto), 5 g L^{-1} NaCl (Sigma), 1 mL L^{-1} *E. coli* sulphur-free salts and 1 mL L^{-1} silicone antifoam (Corning); supplemented post-autoclaving with 5 g L^{-1} glucose and 100 mg L^{-1} carbenicillin. *E. coli* sulphur-free salts comprised 8.2 g $MgCl_2{\cdot}7H_2O$, 1 g $MnCl_2{\cdot}4H_2O$, 0.4 g $FeCl_3{\cdot}6H_2O$, 0.1 g $CaCl_2$, and 2 mL concentrated HCl in 100 mL of distilled water. CheY–GFP production was induced by the addition of 8 μM IPTG at an OD_{650} of around 0.5. Five hours post-induction, 1 mM serine, 1 mM threonine, and 1 mM asparagine were added to the bioreactor. The feed for protocol A contained 100 g L^{-1} tryptone, 50 g L^{-1} yeast extract, 200 g L^{-1} glucose, 10 mM serine, 10 mM threonine, 10 mM asparagine, 100 mg L^{-1} carbenicillin, 8 μM IPTG, 1 mL L^{-1} *E. coli* sulphur-free salts, and 0.1 % (v/v) silicone antifoam in a final volume of 1 L. Feeding began on depletion of initial carbon source as indicated by an increase in the DOT (~11 h post-induction). The feed rate initially was 13.69 mL h^{-1} and was increased when online monitoring systems (DOT and GC–MS) indicated that the feed rate had become growth-limiting (21.13 mL h^{-1} at 30 h, 27.17 mL h^{-1} at 44.5 h, and 38.0 mL h^{-1} at 49.5 h, feed was exhausted at ~57 h [2]).

Protocols B–E used a semi-defined medium [30]: 14 g L^{-1} $(NH_4)_2SO_4$, 20 g L^{-1} yeast extract, 2 g L^{-1} KH_2PO_4, 16.5 g L^{-1} K_2HPO_4, 7.5 g L^{-1} citric acid, 1.5 mL L^{-1} concentrated H_3PO_4, and 0.66 mL L^{-1} polypropylene glycol as antifoam; supplemented post-autoclaving with 34 mL L^{-1} trace metal solution, 10 mM $MgSO_4{\cdot}7H_2O$, 2 mM $CaCl_2{\cdot}2H_2O$, and 100 mg L^{-1} carbenicillin. Protocols B–D used 35 g L^{-1} glycerol as a carbon source; protocol E used 5 g L^{-1} glucose. Trace metal solution contained 3.36 g L^{-1} $FeSO_4{\cdot}7H_2O$, 0.84 g L^{-1} $ZnSO_4{\cdot}7H_2O$, 0.15 g L^{-1} $MnSO_4{\cdot}H_2O$, 0.25 g L^{-1} $Na_2MoO_4{\cdot}2H_2O$, 0.12 g L^{-1} $CuSO_4{\cdot}5H_2O$, 0.36 g L^{-1} H_3BO_3, and 48 mL L^{-1} concentrated H_3PO_4. The feed composition and rate for protocols B–E are described in Table 1. For protocol D, feeding began prior to depletion of carbon source (17.5 h post-induction), was paused to allow consumption of glycerol (18.5 h) and resumed once it was apparent that the glycerol had been consumed (22 h). For protocol E, an exponential feed profile was calculated using the following equation [23]:

$$F = \left(\frac{1}{S}\right) \times \left(\frac{\mu}{Y_{XS}} + m\right) \times X_0 \times e^{\mu t}$$

where: F equals the feed rate into the bioreactor (L h^{-1}), X_0 total biomass in bioreactor at start of feed (g DCW), μ specific growth rate set at 0.2 h^{-1}, t time (h), S feed glucose concentration (400 g L^{-1}), Y_{XS} cell yield on glucose (0.622 g biomass g $glucose^{-1}$ [28]), and m maintenance coefficient for glucose (0.00468 g glucose g $biomass^{-1}$ h^{-1} [28]). A μ of 0.2 was chosen as it is in the range of initial μ values observed (0.05–0.25) for glycerol fermentations in this study. When the feed rate F reached 67.5 mL h^{-1} (at ~25.6 h post-induction), it was not increased any further.

Flow cytometry

Bacteria were analysed using a BD Accuri C6 flow cytometer (BD, Oxford, UK). Samples were excited using a 488 nm solid state laser and fluorescence was detected using 533/30 BP (FL1 channel) and 670 LP (FL3 channel) filters corresponding to GFP and propidium iodide (PI) fluorescence, respectively. Bacteria were stained with PI to determine viability; PI can only enter dead bacteria. A 200 μg PI mL^{-1} stock solution was made up in distilled water and added to samples at a final concentration of 4 μg PI mL^{-1}. Particulate noise was eliminated using a FSC-H threshold. 20,000 data points were collected at a maximum rate of 2,500 events s^{-1}. Data were analysed using CFlow (BD). Percentages of GFP^+ (productive) bacteria were determined using a gate on a FSC-A versus FL1-A intensity plot. Percentages of PI^+ (dead) bacteria were determined using a gate on a FL3-A versus FL1-A intensity plot.

SDS-PAGE

Proteins were separated according to molecular weight using Tris/Glycine SDS-PAGE with a 15 % (w/v) polyacrylamide gel [18]. Bacterial cell pellets were suspended in sample buffer containing β-mercaptoethanol and heated at 100 °C for 10 min before being loaded onto the gel.

Table 1 Summary of fermentation protocols

	A: original improved protocol	B: industrially derived, standard conditions	C: industrially derived, improved conditions	D: industrially derived, improved conditions, mid logarithmic induction, glycerol	E: industrially derived, improved conditions, mid logarithmic induction, glucose
Growth medium	Complex [20]	Semi-defined [30]	Semi-defined [30]	Semi-defined [30]	Semi-defined [30]
Carbon source in batch phase	5 g L^{-1} glucose	35 g L^{-1} glycerol	35 g L^{-1} glycerol	35 g L^{-1} glycerol	5 g L^{-1} glucose
Feed composition and volume	1 L; 100 g L^{-1} tryptone	0.5 L	0.5 L	0.5 L	0.5 L
	50 g L^{-1} yeast extract	714 g L^{-1} glycerol	714 g L^{-1} glycerol	714 g L^{-1} glycerol	400 g L^{-1} glucose
	200 g L^{-1} glucose	7.4 g L^{-1} $MgSO_4 \cdot 7H_2O$	7.4 g L^{-1} $MgSO_4 \cdot 7H_2O$	7.4 g L^{-1} $MgSO_4 \cdot 7H_2O$	7.4 g L^{-1} $MgSO_4 \cdot 7H_2O$
	10 mM each serine, threonine, asparagine				
	100 mg L^{-1} carbenicillin, 8 μM IPTG, 1 mL L^{-1} *E. coli* sulphur-free salts				
	0.1 % (v/v) silicone antifoam				
Feed rate	Stepped (see "Materials and methods")	67.5 mL h^{-1}	67.5 mL h^{-1}	67.5 mL h^{-1}	Exponential at $\mu = 0.2$, up to 67.5 mL h^{-1}
Feed start	On glucose exhaustion	$OD_{650} \approx 40$–50	$OD_{650} \approx 40$–50	On glycerol exhaustion	On glucose exhaustion
Temperature	25 °C	37 °C	25 °C	25 °C	25 °C
IPTG	8 μM	100 μM	8 μM	8 μM	8 μM
Induction point	Mid-logarithmic phase ($OD_{650} \approx 0.5$)	With feeding ($OD_{650} \approx 40$–50)	With feeding ($OD_{650} \approx 40$–50)	Mid-logarithmic phase ($OD_{650} \approx 0.5$)	Mid-logarithmic phase ($OD_{650} \approx 0.5$)

Equal quantities of biomass were loaded into each lane. SDS-PAGE gels were stained with Coomassie Blue and dried, and then scanned (Canon Canoscan 9000F) and the density of each protein band quantified using ImageJ [19] to permit calculation of the percentage of total protein that was CheY–GFP. Independently, soluble and insoluble bacterial protein fractions were separated using BugBuster® (Novagen). Bacterial cell pellets were suspended in a volume of BugBuster® equal to that of sample buffer, incubated at room temperature for 10 min then fractionated by centrifugation at 16,873*g* for 20 min. The pelleted insoluble fraction was subsequently washed in PBS to remove any residual soluble protein. Both fractions were then resuspended in a volume of sample buffer equal to the volume of BugBuster® used and incubated at 100 °C for 10 min before separation by SDS-PAGE as above. This protocol results in soluble fractions that are twice the volume and hence half the protein concentration of the insoluble; to ensure gels were loaded with samples from an equivalent biomass twice the volume of soluble fractions were loaded on the gel. ImageJ was used to determine the percentage of CheY–GFP in the soluble and insoluble fractions.

Results and discussion

This study investigated the production of the CheY–GFP fusion protein, a model 'difficult' protein that is prone to misfolding and inclusion body formation when overexpressed in *E. coli* [8]. CheY is an *E. coli* chemotaxis protein, and is fused here to the commonly used *Aequorea victoria* green fluorescent protein (GFP). Previous studies have demonstrated that GFP fluorescence correlates to correct folding of the CheY–GFP fusion, so can be used as a measure of protein solubility and yield [20, 27]. The genes encoding CheY–GFP are carried by a pET vector [24]; expression is dependent upon the IPTG-inducible T7 RNA polymerase gene encoded at the DE3 locus of the *E. coli* BL21* host. Initial fermentations followed the 'improved' protocol described by Sevastsyanovich et al. [20], referred to here as protocol A (Table 1). Growth data, measured using optical density at 650 nm, reveal that growth proceeded for 48 h post-induction (Fig. 1a) up to an OD_{650} of around 71. Feeding started 11 h after induction, triggered by an increase in DOT (Supplemental Fig. 1) indicating depletion of initial batch phase carbon source (5 g L^{-1} glucose). Peak biomass concentration as determined by DCW analysis was 30.1 g L^{-1}.

Plasmid retention as determined by both replica plating and the GFP^+ phenotype of bacterial colonies on agar plates remained above 94 and 97 %, respectively (Fig. 1b). We also used FCM [13] to determine the green fluorescence of each bacterium; these data are presented as the percentage of bacteria containing GFP (determined by applying a green fluorescence/forward scatter gate, within which bacteria are considered to be GFP^+) and the mean green fluorescence of GFP^+ cells, denoted FL1-A (Fig. 1c). The percentage of GFP^+ cells as determined by FCM remained above 90 % (Fig. 1b), closely correlating with agar plate data. Less than 5 % of bacteria were dead throughout the fermentation as determined by FCM and propidium iodide staining. Online gas MS data (Supplementary Fig. 1) reveal that oxygen demand and CO_2 evolution rates dropped sharply after around 55 h post-induction, corresponding to the end of the feed.

The mean green fluorescence of CheY–GFP^+ bacteria (FL1-A, determined using FCM) increased over the course of the fermentation following a small decrease immediately post-induction (Fig. 1c), thought to be caused by a concurrent decrease in bacterial size [as indicated using FCM forward scatter (FSC-A) measurements]. The cell size dynamics observed here are concomitant with previous studies of *E. coli* cell size over growth curves; an increase in cell size during lag phase, followed by a decrease in cell size during exponential growth [1].

Maximum green fluorescence per bacterium did not increase significantly after 28 h post-induction, although biomass increased thus increasing the quantity of recombinant protein present in the fermenter as a whole. SDS-PAGE analysis of whole bacteria and soluble and insoluble bacterial fractions (Fig. 1d) revealed that CheY–GFP concentration per unit biomass (expressed as a percentage of whole cell protein) did not dramatically change during the fermentation, increasing slightly from 11.4 % at induction to 16.8 % at 24 h post-induction, then fluctuated over the remainder of the fermentation. The percentage of CheY–GFP in the soluble fraction (as determined by Bugbuster® extraction) did increase from around 40 % soluble at induction to over 60 % soluble 26 h post-induction; this increase occurred at the same time as the increase in green fluorescence as measured by FCM.

Taken together, the protocol A fermentation could therefore be split into three phases: 0–28 h post-induction, concurrent increase in biomass and quantity of recombinant protein per cell; 28–48 h, biomass accumulation but no change in quantity of CheY–GFP per cell; and accumulation of neither biomass nor recombinant protein after 48 h post-induction. 48 h could be determined to be the optimal harvest time. The final yield of total CheY–GFP produced (at 70 h post-induction) was estimated to be 2.3 g L^{-1} (assuming protein comprises 60 % of DCW, based on observations of 50–61 % [26] and an estimate of 70 % by Sevastsyanovich et al. [20]), corresponding to a yield of 1.5 g L^{-1} soluble CheY–GFP.

Three potential problems were identified with protocol A [20] that could limit its utility in biopharmaceutical

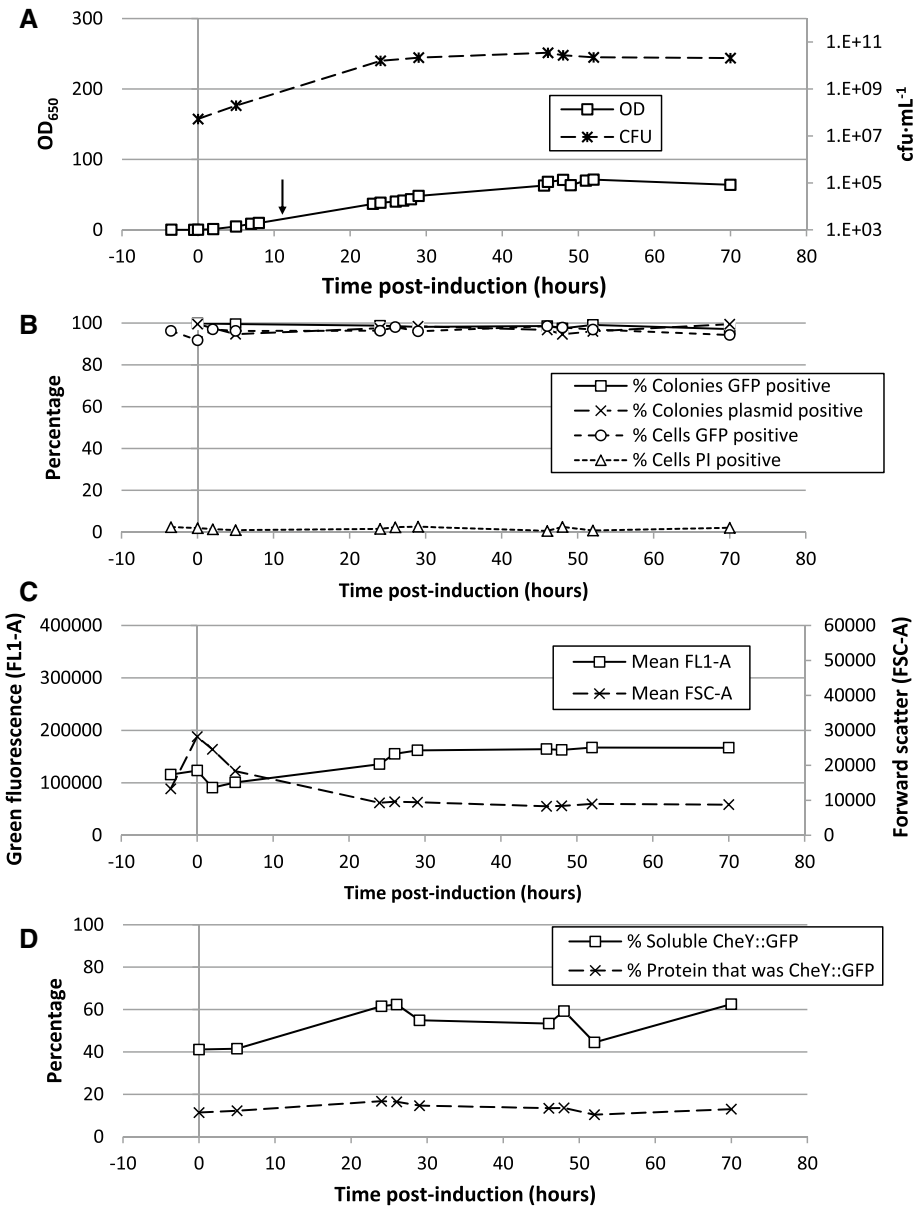

Fig. 1 Fermentation data using protocol A (original 'improved' protocol, complex medium and feed, early induction). **a** OD_{650} (*squares*) and CFU (*crosses*) data. *Arrow* indicates time of feed starting. **b** Plasmid retention data; percentage of colonies that were GFP^+ (*squares*) and percentage $plasmid^+$ colonies (*crosses*) as determined using agar plates. Flow cytometry data; percentage of cells that were GFP^+ (*circles*) and percentage of cells that were PI^+ and so dead (*triangles*). **c** Flow cytometry data; mean cellular green fluorescence (FL1-A) of GFP^+ cells (*squares*) and mean forward scatter (FSC-A) of GFP^+ cells (*crosses*). **d** SDS-PAGE data; percentage solubility of CheY–GFP (*squares*) and percentage of total protein that was CheY–GFP (*crosses*). Data from a representative fermentation of a minimum of two replicates

manufacturing. First, both the base medium and feed contain complex animal-derived products (tryptone) so are not suitable for a cGMP process. Many industrial RPP processes tend to use defined media or semi-defined media without animal products; choice of defined or semi-defined media is usually down to company policy and product. The use of semi-defined media offers a compromise before the potentially high cost of development of a fully defined medium optimised for a particular bioprocess. Minimisation of the use of complex media components also decreases the risks of batch variability. This variability was characterised for this system by growing the *E. coli* BL21* pCheY–GFP strain for 14 h at 30 °C in LB medium composed of complex medium components sourced from different suppliers: a variability of 21 % in final OD_{650} was observed due to differences in yeast extract and tryptone composition.

Second, large quantities of additional complex medium components are fed into the fermenter during the fed-batch phase. This can result in osmotic problems and the presence of large quantities of undefined proteinaceous medium components can complicate downstream processing of product proteins [5]. Finally, use of glucose as a feed can present difficulties from acid formation due to overflow metabolism, especially when growth rates fluctuate. Use of glycerol as a carbon source does not usually present this problem. These three concepts in industrial fermentation design are typified by the protocol used by Want et al. [30], which was used to test CheY–GFP expression here (referred to as protocol B; Table 1).

Use of an industrially derived fermentation protocol

As well as the use of semi-defined medium and glycerol as carbon source, protocol B used a growth temperature of 37 °C and induction at a relatively high biomass using a high concentration (0.1 mM) of IPTG. The glycerol feed was started at the same time as induction, when online measurements suggested exhaustion of batch-phase glycerol (primarily by reduction in oxygen demand), and was fed at a rate of 67.5 mL h^{-1}. This protocol resulted in more heterogenous data than protocol A; data from two fermentations are shown in Fig. 2. The growth data in terms of OD_{650} and CFU measurements are similar for both fermentations (Fig. 2a). Cell density increased to an OD_{650} of around 55, whereupon RPP was induced by addition of 0.1 mM IPTG. Growth continued until an OD_{650} of around 80; oxygen consumption data (DOT and gas MS) reveal that induction caused growth arrest followed by a recovery, but rapid growth only proceeded for around 5 h post-induction (Supplementary Fig. 2). This is indicative of metabolic stress generated upon CheY–GFP synthesis at 37 °C [20].

Although the growth of duplicate fermentations was similar, CheY–GFP production in each fermentation was quite different. Both replicates showed high levels of plasmid loss before induction (as determined both by plating and FCM; Fig. 2b), suggesting that even uninduced cells were under stress. CheY–GFP is synthesised from this plasmid system even in the absence of inducer (Fig. 1), thus imposing stress before induction [20]. FCM data revealed that 15 h post-induction, >30 % of bacteria were still CheY–GFP^+ in fermenter 1; despite this, on agar plates, all colonies from fermenter 1 were GFP^- at this time point. This is likely caused by physiological stress in CheY–GFP^+ bacteria generating a viable but non-culturable phenotype, commonly encountered in bacterial recombinant protein production cultures. Plasmid loss was greater in fermentation 2 than 1; only ≈10 % of bacteria were CheY–GFP^+. The proportion of dead (PI^+) bacteria in fermenter 1 was also higher than in fermenter 2, and the CFU mL^{-1} was lower. Mean green fluorescence of the CheY–GFP^+ bacteria were equivalent (Fig. 2c), but the much lower proportion of productive bacteria in fermenter 2 meant that far less CheY–GFP was produced per unit biomass (Fig. 2d). It is interesting to note that the solubility of CheY–GFP produced by fermenter 2 was very high; this is probably a consequence of the very low quantity of CheY–GFP being produced.

For fermenter 1, the final yield of CheY–GFP was estimated at 2.2 g L^{-1}, corresponding to a yield of 0.7 g L^{-1} soluble CheY–GFP. It can be concluded that fermenter 1 was more productive in terms of CheY–GFP productivity per unit biomass, but that bacteria were under greater physiological stress. Fermenter 2 had a lower proportion of productive bacteria, resulting in a lower CheY–GFP yield (≈0.6 g L^{-1} CheY–GFP, ≈0.5 g L^{-1} soluble CheY–GFP) but less physiological stress, resulting in higher CFU measurements and a lower proportion of dead bacteria.

The low overall levels of plasmid retention, green fluorescence, and CheY–GFP accumulation and solubility as compared to protocol A suggests that protocol B put bacteria under physiological stress that was detrimental to recombinant protein production. Therefore, the improvements used to initially design the improved protocol A were applied to the industrially derived protocol B; namely reduction of temperature to 25 °C throughout and induction with a far lower concentration of IPTG (8 μM) to generate protocol C (Table 1).

Application of improved conditions to an industrial protocol

Due to the low growth temperature compared to protocol B, protocol C cultures grew far slower (Fig. 3a), taking around 21 h to reach the induction point (OD_{650} ≈ 40, when glycerol was exhausted as indicated by online measurements). Following induction, the culture grew well for 11 h as indicated by a steady increase in oxygen demand (DOT and gas MS data; Supplementary Fig. 3). The feed likely became growth limiting at 11 h post-induction, even though it lasted until around 18 h post induction, at which point oxygen demand (as determined by gas MS) fell dramatically. The final OD_{650} was recorded as 297. Unlike protocol B cultures, the proportion of GFP^+ bacteria as measured by FCM remained very high throughout (>93 %), indicative of good plasmid retention and a consequence of lowered physiological stress (Fig. 3b). Mean green fluorescence per GFP^+ bacterium as determined by FCM (FL1-A) decreased between inoculation and induction (concurrent with a decrease in cell size, signified by mean FSC-A measurements) and, as in protocol A, increased following induction, although this increase was to a far greater extent than protocol A cultures, reaching a peak mean green fluorescence of 240,000 compared to 176,000 for protocol A (Fig. 3c). Unlike protocol A cultures, mean forward scatter (FSC-A), signifying bacterial size, increased following induction, and was greater at the end of the fermentation in protocols B and C than in protocol A. This is probably due to the higher osmolarity in the medium and feed used in protocol A [16].

CheY–GFP solubility as determined by Bugbuster® peaked at nearly 60 % at the point of induction and then decreased to a low point at 5 h post-induction, however, recovered to almost the peak value at termination reaching a final solubility of around 56 % (Fig. 3d). Total CheY–GFP accumulation per unit biomass followed a similar pattern, however, peak accumulation occurred at 2 h post-induction. These data suggest that CheY–GFP concentration per unit biomass and solubility were lowest during

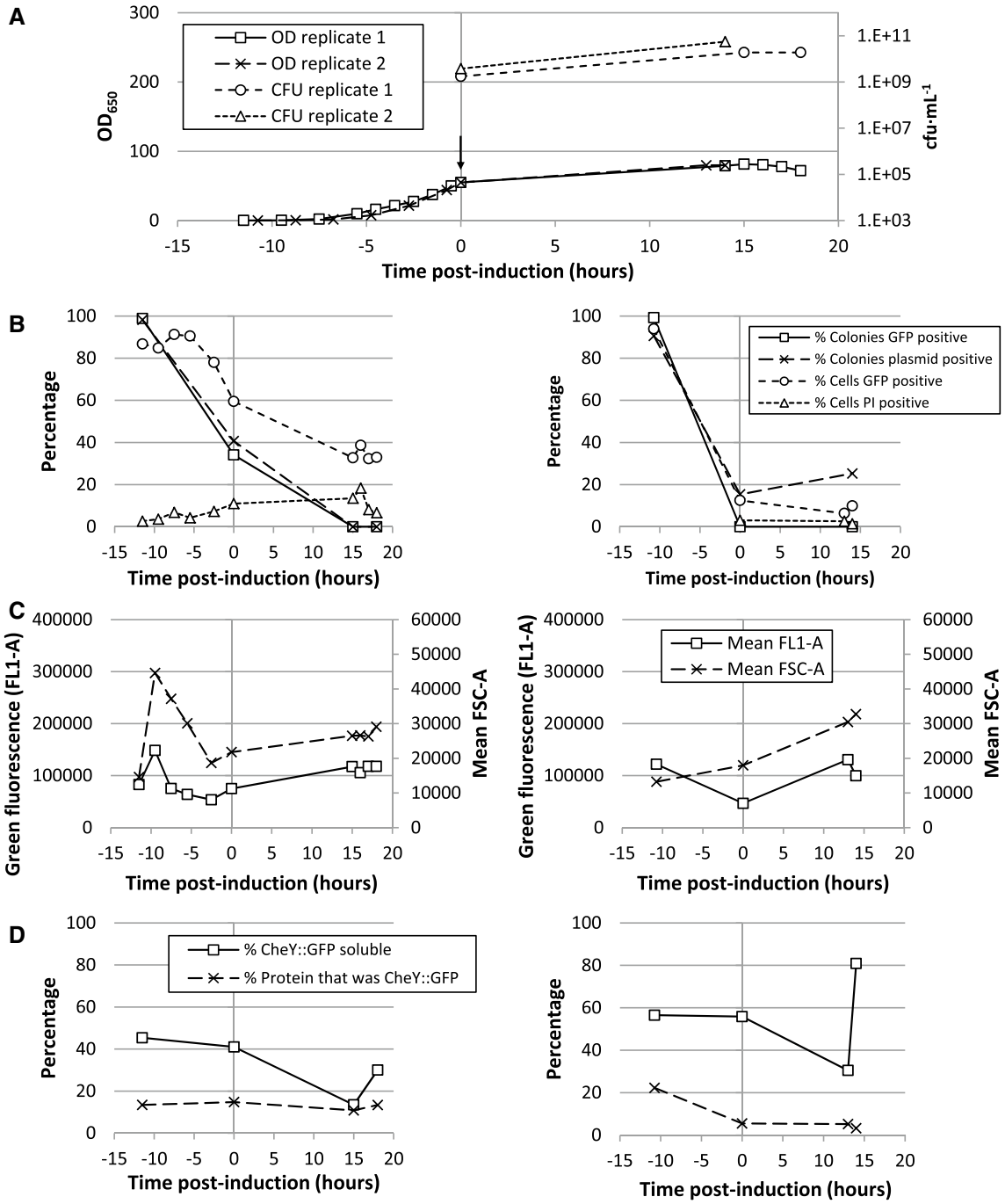

Fig. 2 Fermentation data using protocol B [industrially derived 'standard' conditions, semi-defined medium, late induction, high (IPTG)]. **a** OD_{650} data for replicate 1 (*squares*) and 2 (*crosses*) CFU data for replicate 1 (*circles*) and 2 (*triangles*). *Arrow* indicates time of feed starting. **b** Plasmid retention data; percentage of colonies that were GFP^+ (*squares*) and percentage $plasmid^+$ colonies (*crosses*) as determined using agar plates. Flow cytometry data; percentage of cells that were GFP^+ (*circles*) and percentage of cells that were PI^+ and so dead (*triangles*). Replicate 1—*left*, replicate 2—*right*. **c** Flow cytometry data; mean cellular green fluorescence (FL1-A) of GFP^+ cells (*squares*) and mean forward scatter (FSC-A) of GFP^+ cells (*crosses*). Replicate 1—*left*, replicate 2—*right*. **d** SDS-PAGE data; percentage solubility of CheY–GFP (*squares*) and percentage of total protein that was CheY–GFP (*crosses*). Replicate 1—*left*, replicate 2—*right*

periods of rapid growth. The final yield of CheY–GFP was estimated at 10.7 g L^{-1}, corresponding to a yield of 6 g L^{-1} soluble CheY–GFP.

Summary data comparing protocols B and C (Table 2) clearly demonstrate the benefits of operating using stress-minimisation conditions in terms of the resultant

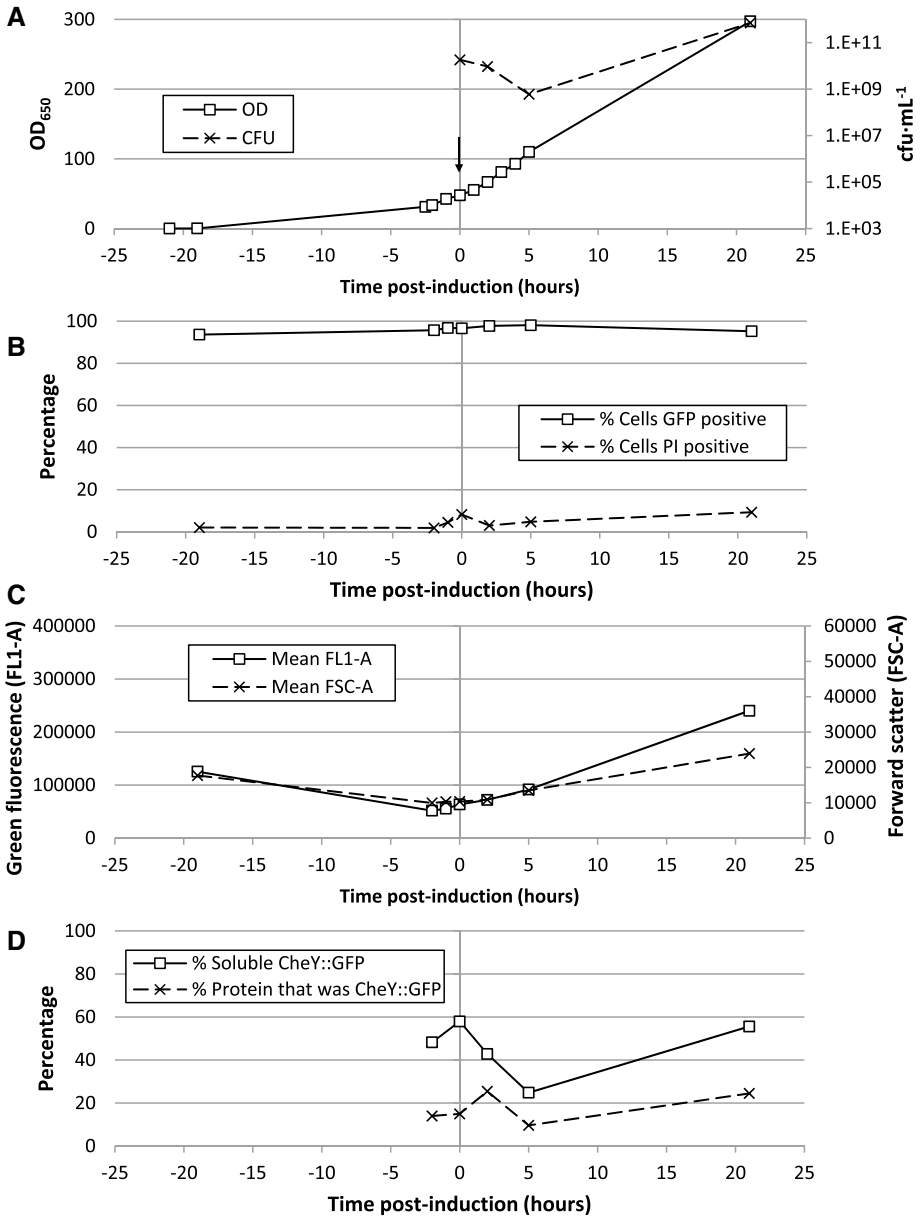

Fig. 3 Fermentation data using protocol C [improved industrially derived conditions, semi-defined medium, late induction, low (IPTG)]. **a** OD_{650} (*squares*) and CFU (*crosses*) data. *Arrow* indicates time of feed starting. **b** Flow cytometry data; percentage of cells that were GFP^+ (*squares*) and percentage of cells that were PI^+ and so dead (*crosses*). **c** Flow cytometry data; mean cellular green fluorescence (FL1-A) of GFP^+ cells (*squares*) and mean forward scatter (FSC-A) of GFP^+ cells (*crosses*). **d** SDS-PAGE data; percentage solubility of CheY–GFP (*squares*) and percentage of total protein that was CheY–GFP (*crosses*). Data from a representative fermentation of a minimum of two replicates

biomass yield (final OD_{650} increased nearly fourfold; DCW increased almost threefold) and recombinant protein yield and solubility. Compared to protocol A, protocol C showed an almost fivefold increase in cell density and although FCM analysis showed similar percentages of GFP^+ cells, suggesting similar levels of plasmid retention, GFP^+ bacteria in protocol C at harvest were 46 % more fluorescent than in protocol A and showed higher levels of homogeneity as evidenced by the lower CV of the green fluorescence values. CheY–GFP solubility as assessed by BugBuster® fractionation was 11 % higher in protocol A than in protocol C; this is in agreement with Moore et al. [12] who showed that increasing the concentration of complex media components (tryptone and yeast extract) increased solubility of recombinant T4 dCMP deaminase. However, CheY–GFP concentration as a percentage of total cellular protein in protocol C was almost double that of protocol A; this may partially explain the slightly lower solubility, the higher quantity of CheY–GFP having overwhelmed the bacterial protein folding pathways. These data, combined with the increased biomass, resulted in an over fourfold increase in CheY–GFP volumetric yield and a fourfold increase in the volumetric yield of soluble CheY–GFP.

Alteration of induction point

As in protocol B [30], many RPP protocols induce recombinant protein production at a relatively high biomass to separate biomass generation and recombinant protein production stages. This is often done when the recombinant

Table 2 Summary of fermentation data at harvest

Protocol	Peak/final OD_{650}[a]	DCW (g L^{-1})	$Y_{X/S}$ (g g^{-1})	Flow cytometry measurements					SDS-PAGE		Total CheY::GFP (g L^{-1})[c]	Total soluble CheY::GFP (g L^{-1})
				% bacteria GFP^+	% bacteria PI^+	Mean FL1-A (GFP^+ bacteria)	Mean FL1-A (all bacteria)	% coefficient of variation (CV) FL1-A	Mean FSC-A (GFP^+ bacteria)	% CheY::GFP soluble	% of protein that is CheY::GFP		
A	64.5 (71.8)	30.1	0.363	94.3	2.1	166,700 (176,100)	157,200	73	8,800	62.5	13.0	2.3	1.5
B[b]	72.4 (81.8)	27.9	0.136	33.0	6.7	117,700 (117,800)	62,800	93	29,100	30.0	13.4	2.2	0.7
C	297	72.8	0.365	95.2	9.3	240,100	228,600	54	23,900	55.6	24.5	10.7	6
D	288	77.5	0.378	73.5	8.8	369,400	271,600	83	25,200	37.4	25.7	12.0	4.5
E	167	42.6	0.411	98.2	5.9	295,500	290,100	73	22,700	49.5	30.1	7.7	3.8

[a] Values in parentheses are peak measurements

[b] Values refer to fermentation 1 (Fig. 2)

[c] Estimated from DCW and % CheY::GFP of total protein assuming protein comprises 60 % of *E. coli* dry cell mass (based on 50–61 % estimates from [26] and 70 % from [20])

protein in question is a 'toxic' protein, prone to cause host bacteria stress; in addition this can lead to reduction in metabolic burden that can be caused by simultaneous requirements for cellular resources for both biomass and recombinant protein generation. For many recombinant protein production processes, the time from induction to time for harvest is limited (the 'production window') and is governed by the amount of time that the host bacteria can generate recombinant protein without losing viability. Protocol A utilised early induction, using the logic that reduction in stress and lower growth rates would allow bacteria to generate recombinant protein more slowly and thus apportion cellular resources more evenly between biomass and recombinant protein generation. Therefore, protocol C was modified to allow induction at an earlier point ($OD_{650} \approx 0.5$), as in protocol A, to generate protocol D.

Cell growth was broadly comparable to protocol C, taking around 40 h to reach an OD_{650} of 288 (Fig. 4a). Online data revealed that metabolic activity declined at 28 h post-induction (Supplementary Fig. 4), reflecting a decrease in growth rate; as with protocol C, this is probably due to the feed rate limiting growth. The proportion of GFP^+ cells as determined by FCM (Fig. 4b) during early stages of the fermentation was lower than expected at ~80 %; however, this was mainly due to non-fluorescent antifoam particulate matter with a similar scatter distribution to bacteria; this particulate noise was visible due to a low cell density at the start of these fermentations. At later points in the fermentation the percentage of GFP^+ cells remained above 95 % but at termination the proportion had dropped to 74 %. PI staining also showed an increase in the percentage of dead cells at termination up to 8.8 %. These data suggest that by termination the culture had become physiologically stressed. As before, the mean green fluorescence of GFP^+ bacteria and the mean forward scatter initially decreased (Fig. 4c); after 18 h post-induction both parameters steadily increased until termination, FL1-A reaching a final value of 370,000. The increase in FL1-A during the latter stages of the fermentation was greater than that of FSC-A (signifying cell size), suggesting accumulation of CheY–GFP per bacterium. FSC-A changes were similar to protocol C, except that induction occurred at the maximum mean FSC-A value rather than the minimum; this suggests that bacterial size is primarily regulated in response to growth phase and is not a result of recombinant protein production. SDS-PAGE analysis (Fig. 4d) showed a steady increase in the percentage of total cellular protein that was CheY–GFP throughout; from 16 % at the point of induction to 26 % at termination. However, the percentage solubility showed an overall decrease during the fermentation from 47 % at induction to 37 % at termination, suggesting that overall product quality had decreased; again, possibly due to higher rates of CheY–GFP synthesis, as seen in protocol C.

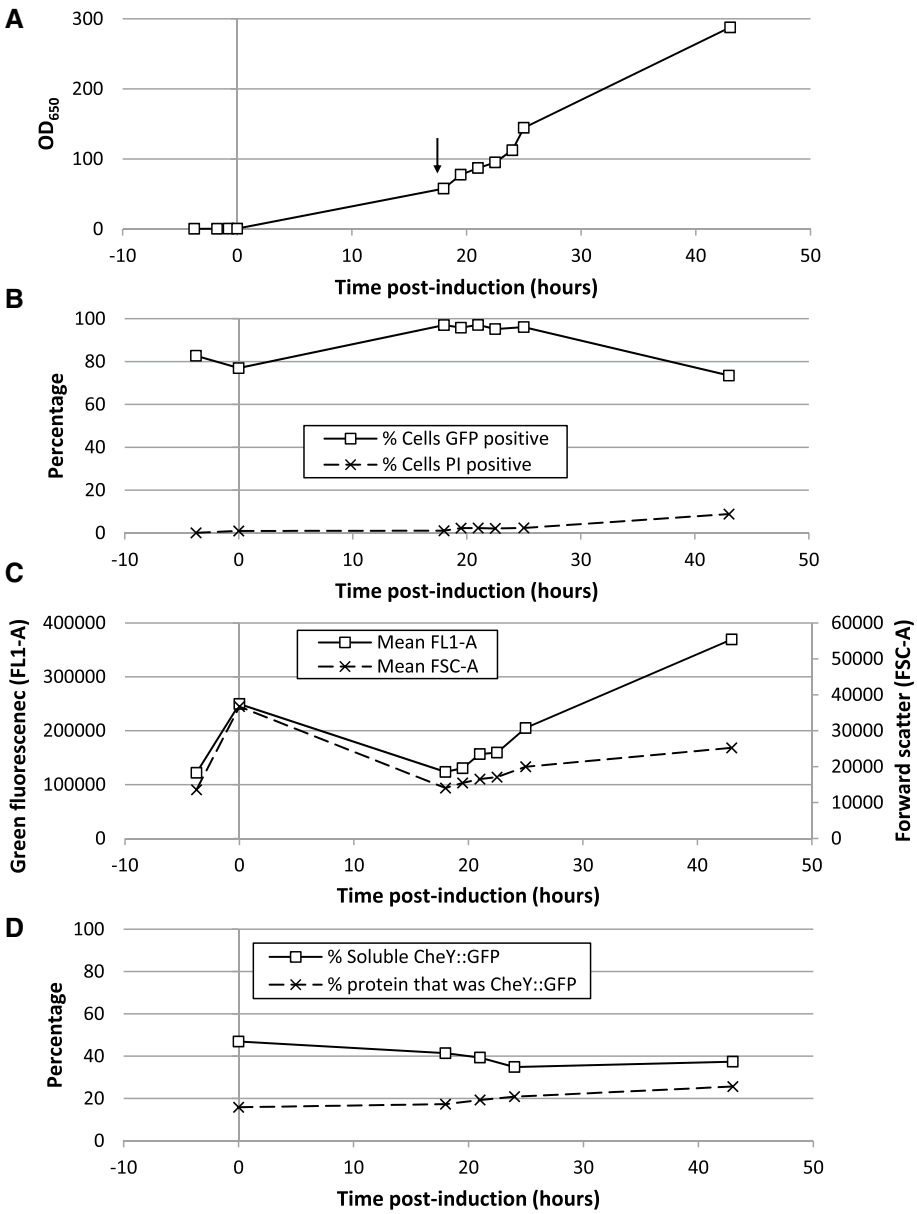

Fig. 4 Fermentation data using protocol D [improved industrially derived conditions, semi-defined medium, early induction, low (IPTG)]. **a** OD_{650} (*squares*) data. *Arrow* indicates time of feed starting. **b** Flow cytometry data; percentage of cells that were GFP^+ (*squares*) and percentage of cells that were PI^+ and so dead (*crosses*). **c** Flow cytometry data; mean cellular green fluorescence (FL1-A) of GFP^+ cells (*squares*) and mean forward scatter (FSC-A) of GFP^+ cells (*crosses*). **d** SDS-PAGE data; percentage solubility of CheY–GFP (*squares*) and percentage of total protein that was CheY–GFP (*crosses*). Data from a representative fermentation of a minimum of two replicates

Final yield of CheY–GFP was estimated at 12 g L^{-1}, corresponding to a yield of 4.5 g L^{-1} soluble CheY–GFP.

Comparing protocols C and D allow the effect of early versus late induction to be examined. In terms of biomass generation protocols C and D showed similar final measurements (Table 2). In addition, culture viability, as indicated by the percentage of PI^+ cells, was similar. It can therefore reasonably be concluded that culture growth and biomass generation did not appear to be affected by earlier induction. In terms of CheY–GFP productivity the effect of early induction was an increase in heterogeneity within the culture. The percentage of total protein that was CheY–GFP was similar at harvest, but the product quality, as indicated by CheY–GFP solubility, was almost 20 % lower in protocol D. The proportion of GFP^+ cells was over 20 % lower for protocol D, but the mean green fluorescence of the GFP^+ cells was over 50 % higher. Nonetheless, similar amounts of CheY–GFP per unit biomass were observed by SDS-PAGE in protocols C and D, although its solubility was lower in protocol D.

Based on these data, earlier induction increased culture heterogeneity in protocol D, evidenced by a larger number of GFP^- cells, and a lower percentage of soluble CheY–GFP as determined by SDS-PAGE. It is possible that induction of RPP tends to select for culture heterogeneity, even in stress-minimising conditions; the longer time between induction and harvest allowed a larger subpopulation to develop in protocol D than protocol C. This represents an additional factor when choosing a harvest window.

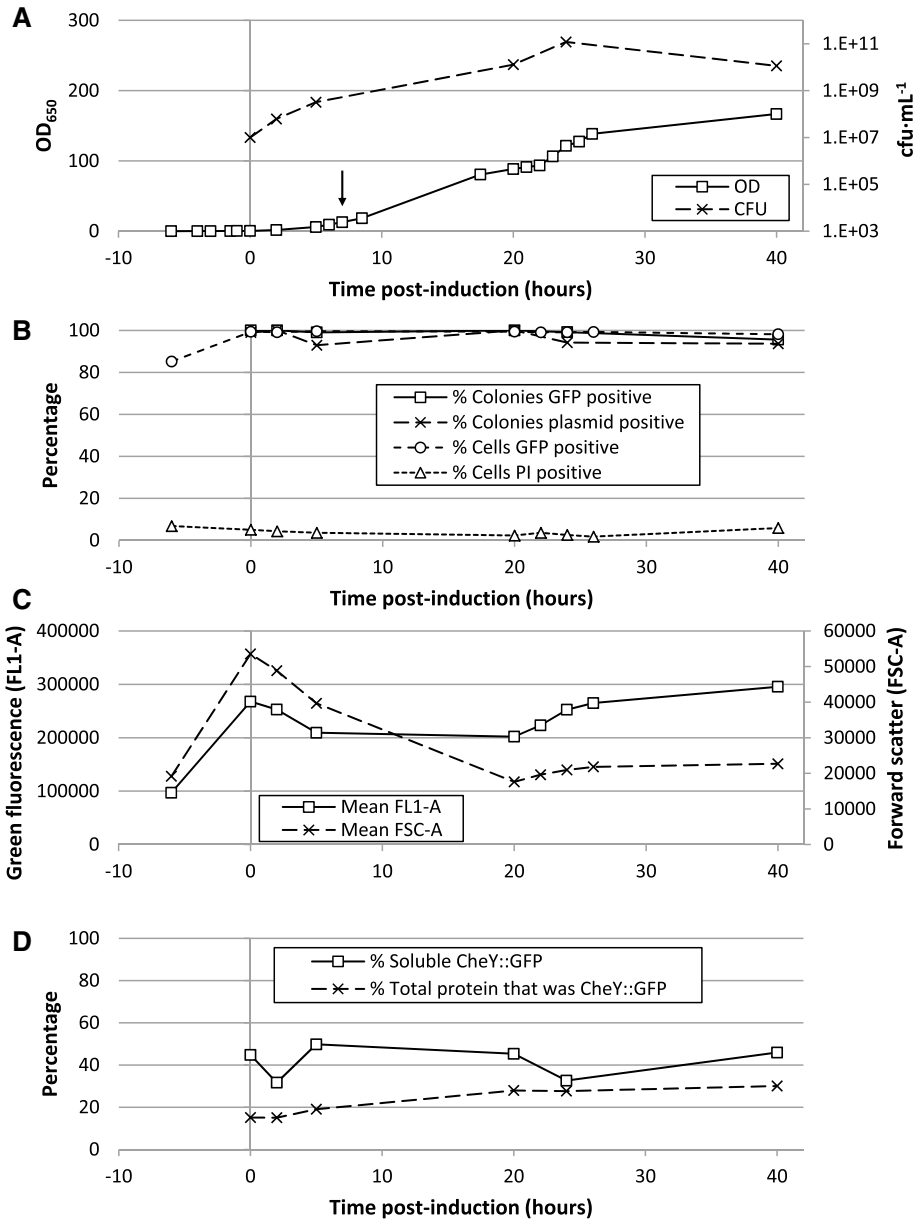

Fig. 5 Fermentation data using protocol E [improved industrially derived conditions, semi-defined medium, early induction, low (IPTG), glucose feed]. **a** OD_{650} (*squares*) and CFU (*crosses*) data. *Arrow* indicates time of feed starting. **b** Plasmid retention data; percentage of colonies that were GFP^+ (*squares*) and percentage $plasmid^+$ colonies (*crosses*) as determined using agar plates. Flow cytometry data; percentage of cells that were GFP^+ (*circles*) and percentage of cells that were PI^+ and so dead (*triangles*). **c** Flow cytometry data; mean cellular green fluorescence (FL1-A) of GFP^+ cells (*squares*) and mean forward scatter (FSC-A) of GFP^+ cells (*crosses*). **d** SDS-PAGE data; percentage solubility of CheY–GFP (*squares*) and percentage of total protein that was CheY–GFP (*crosses*). Data from a representative fermentation of a minimum of two replicates

Use of glucose as a carbon source

Although glycerol has advantages over glucose as a carbon source, it is more expensive and the preferred carbon and energy source of *E. coli* is glucose. Therefore, protocol D was modified to use glucose as a carbon source both in the batch medium and the feed, generating protocol E. Growth data reveal steady growth to a final OD_{650} of 167 (Fig. 5a); gas MS revealed that growth significantly slowed at 32 h post-induction (Supplemental Fig. 5), corresponding to the end of the glucose feed. Plasmid retention remained above 92 % throughout (Fig. 5b). The percentage of GFP^+ cells determined by FCM remained above 98 %, except for the initial sample that was 85 %, again caused by antifoam particulates. The percentage of dead cells as determined by FCM remained at <7 % throughout, although there was an increase between 26 h (1.8 %) and termination (5.9 %), possibly suggesting a increase in cell stress due to the onset of stationary phase.

Mean green fluorescence and forward scatter of GFP^+ cells (Fig. 5c) showed a similar pattern to other early-induced fermentations. Between 6 and 20 h post-induction FSC-A decreased to a greater extent than FL1-A, suggesting that while the cells became smaller, CheY–GFP content per cell increased. Between 20 and 26 h post-induction FL1-A increased by ~30 % and FSC-A increased by ~20 %, suggesting accumulation of CheY–GFP per cell despite increasing cell size. At termination mean green

fluorescence per bacterium had reached 296,000. SDS-PAGE data (Fig. 5d) showed an increase in the percentage of total cellular protein that was CheY–GFP from 2 h post-induction until termination, reaching a final peak value of 30 %. CheY–GFP solubility fluctuated during the fermentation, the peak solubility of 50 % being observed at 5 h post-induction and final solubility being 46 %. Final yield of CheY–GFP was estimated at 7.7 g L^{-1}, corresponding to a yield of 3.8 g L^{-1} soluble CheY–GFP.

Although utilising the same carbon source, protocol E shows several benefits over protocol A: a 2.5-fold increase in OD_{650}; a 65 % increase in the mean green fluorescence of GFP^+ bacteria; and the largest amount of CheY–GFP as expressed as a percentage of cellular protein achieved in this study. Although the soluble percentage of CheY–GFP was higher in protocol A than protocol E, the far higher quantity of CheY–GFP per cell and higher biomass concentration meant that the volumetric yield of soluble CheY–GFP in protocol E was over double that of protocol A (3.8 g L^{-1} versus 1.5 g L^{-1}). As before, increases in CheY–GFP per cell probably correlate with decreases in CheY–GFP solubility due to overloading of cellular protein folding pathways.

Comparison of protocols E and D allows elucidation of differences caused by changing carbon source. There are numerous studies that claim recombinant protein production is enhanced by growth on either glucose [3, 25] or glycerol [9, 15, 31]; this seems to be dependent upon recombinant protein, strain, medium composition, and growth conditions, and so is likely not a generic effect. In this study, protocol E had a lower final OD_{650} than D; however, this was expected as total glucose added was less than glycerol, and $Y_{X/S}$ values were broadly comparable (Table 2). FCM data demonstrate that there were fewer GFP^- bacteria in protocol E than D, suggesting lower physiological stress, although protocol D had a longer runtime than E, which could select for a non-productive GFP^- subpopulation. CheY–GFP yield per cell and solubility were higher in protocol E, although the higher biomass generated in protocol D resulted in a higher overall CheY–GFP yield. Again, there is a balance between biomass production, CheY–GFP production and solubility; protocols C–E have demonstrated that although each of these parameters may be optimised individually, it is at the expense of other parameters.

Conclusion

The stress-minimisation method [20] has been shown to be highly applicable to an industrially derived high cell density fed-batch recombinant protein production protocol, both with early and late induction of RPP and with glucose and glycerol as carbon sources. Stress minimisation increased biomass yield and CheY–GFP yield and solubility while decreasing culture heterogeneity. Similarly, transfer to a semi-defined medium improved biomass yield and overall CheY–GFP productivity per unit volume, while representing a more industrially favoured approach to RPP due to elimination of animal-derived products and minimisation of complex media components. Changing the point of induction was shown to have little overall effect on the improved protocols. FCM was shown to be a very useful analytical tool in fermentation monitoring and optimisation, in particular allowing culture heterogeneity, stress and the relationship between bacterial size and GFP content to be monitored. In summary, the stress-minimisation methods described here could effectively be applied to a wide range of high cell density culture recombinant protein production fermentations.

Acknowledgements This work was supported by a UK Biotechnology and Biological Sciences Research Council PhD studentship to CW. We thank Yanina Sevastsyanovich and Tania Selas Castiñeiras for helpful comments on the manuscript.

Conflict of interest The BD Accuri C6 flow cytometer was awarded to TWO by the BD Accuri Creativity Award. TWO was paid speakers expenses by BD for speaking at a BD Accuri users' event. The funders played no role in the design or implementation of this study.

References

1. Åkerlund T, Nordström K, Bernander R (1995) Analysis of cell size and DNA content in exponentially growing and stationary-phase batch cultures of *Escherichia coli*. J Bacteriol 177:6791–6797
2. Alfasi S, Sevastsyanovich Y, Zaffaroni L, Griffiths L, Hall R, Cole J (2011) Use of GFP fusions for the isolation of *Escherichia coli* strains for improved production of different target recombinant proteins. J Biotechnol 156:11–21
3. Carvalho RJ, Cabrera-Crespo J, Tanizaki MM, Goncalves VM (2012) Development of production and purification processes of recombinant fragment of pneumococcal surface protein A in *Escherichia coli* using different carbon sources and chromatography sequences. Appl Microbiol Biotechnol 94:683–694
4. Cormack BP, Valdivia RH, Falkow S (1996) FACS-optimized mutants of the green fluorescent protein (GFP). Gene 173:33–38
5. Cote RJ (2010) Media composition, microbial, laboratory scale. In: Flickinger MC (ed) Encyclopedia of industrial biotechnology, bioprocess, bioseparation, and cell technology. Wiley, New York, pp 3277–3297
6. García-Fruitós E, González-Montalbán N, Morell M, Vera A, Ferraz RM, Arís A, Ventura S, Villaverde A (2005) Aggregation as bacterial inclusion bodies does not imply inactivation of enzymes and fluorescent proteins. Microb Cell Fact 4:27
7. Jones JJ, Bridges AM, Fosberry AP, Gardner S, Lowers RR, Newby RR, James PJ, Hall RM, Jenkins O (2004) Potential of real-time measurement of GFP-fusion proteins. J Biotechnol 109:201–211
8. Jones JJ (2007) Green fluorescent protein as an analytical tool to dissect the physiology of recombinant protein production in fermenters. PhD thesis, University of Birmingham, Birmingham

9. Luo Q, Shen YL, Wei DZ, Cao W (2006) Optimization of culture on the overproduction of TRAIL in high-cell-density culture by recombinant *Escherichia coli*. Appl Microbiol Biotechnol 71:184–191
10. Martínez-Alonso M, García-Fruitós E, Ferrer-Miralles N, Rinas U, Villaverde A (2010) Side effects of chaperone gene co-expression in recombinant protein production. Microb Cell Fact 9:64
11. Miroux B, Walker JE (1996) Over-production of proteins in *Escherichia coli*: mutant hosts that allow synthesis of some membrane proteins and globular proteins at high levels. J Mol Biol 260:289–298
12. Moore JT, Uppal A, Maley F, Maley GF (1993) Overcoming inclusion body formation in a high-level expression system. Protein Expr Purif 4:160–163
13. Müller S, Nebe-von-Caron G (2010) Functional single-cell analyses: flow cytometry and cell sorting of microbial populations and communities. FEMS Microbiol Rev 34:554–587
14. Overton TW (2014) Recombinant protein production in bacterial hosts. Drug Discov Today (in press). doi:10.1016/j.drudis.2013.11.008
15. Pflug S, Richter SM, Urlacher VB (2007) Development of a fed-batch process for the production of the cytochrome P450 monooxygenase CYP102A1 from *Bacillus megaterium* in *E. coli*. J Biotechnol 129:481–488
16. Reuter M, Hayward NJ, Black SS, Miller S, Dryden DT, Booth IR (2013) Mechanosensitive channels and bacterial cell wall integrity: does life end with a bang or a whimper? J R Soc Interface 11:20130850. doi:10.1098/rsif.2013.0850
17. Saïda F, Uzan M, Odaert B, Bontems F (2006) Expression of highly toxic genes in *E. coli*: special strategies and genetic tools. Curr Protein Pept Sci 7:47–56
18. Sambrook J, Fritsch EF, Maniatis T (1987) Molecular cloning: a laboratory manual, 2nd edn. Cold Spring Harbor Press, Cold Spring Harbor, NY
19. Schneider CA, Rasband WS, Eliceiri KW (2012) NIH Image to ImageJ: 25 years of image analysis. Nat Methods 9:671–675
20. Sevastsyanovich Y, Alfasi S, Overton T, Hall R, Jones J, Hewitt C, Cole J (2009) Exploitation of GFP fusion proteins and stress avoidance as a generic strategy for the production of high-quality recombinant proteins. FEMS Microbiol Lett 299:86–94
21. Singh SM, Panda AK (2005) Solubilization and refolding of bacterial inclusion body proteins. J Biosci Bioeng 99:303–310
22. Sørensen HP, Mortensen KK (2005) Soluble expression of recombinant proteins in the cytoplasm of *Escherichia coli*. Microb Cell Fact 4:1
23. Strandberg L, Andersson L, Enfors S (1994) The use of fed batch cultivation for achieving high cell densities in the production of a recombinant protein in *Escherichia coli*. FEMS Microbiol Rev 14:53–56
24. Studier FW (1991) Use of bacteriophage T7 lysozyme to improve an inducible T7 expression system. J Mol Biol 219:37–44
25. Tseng CL, Leng CH (2012) Influence of medium components on the expression of recombinant lipoproteins in *Escherichia coli*. Appl Microbiol Biotechnol 93:1539–1552
26. Valgepea K, Adamberg K, Seiman A, Vilu R (2013) *Escherichia coli* achieves faster growth by increasing catalytic and translation rates of proteins. Mol BioSyst 9:2344–2358
27. Waldo GS, Standish BM, Berendzen J, Terwilliger TC (1999) Rapid protein-folding assay using green fluorescent protein. Nat Biotechnol 17:691–695
28. Wallace R, Holms W (1986) Maintenance coefficients and rates of turnover of cell material in *Escherichia coli* ML308 at different growth temperatures. FEMS Microbiol Lett 37:317–320
29. Walsh G (2010) Biopharmaceutical benchmarks. Nat Biotechnol 28:917–924
30. Want A, Thomas OR, Kara B, Liddell J, Hewitt CJ (2009) Studies related to antibody fragment (Fab) production in *Escherichia coli* W3110 fed-batch fermentation processes using multiparameter flow cytometry. Cytom A 75:148–154
31. Zhang JD, Li AT, Xu JH (2010) Improved expression of recombinant cytochrome P450 monooxygenase in *Escherichia coli* for asymmetric oxidation of sulfides. Bioprocess Biosyst Eng 33:1043–1049